

Publisher: GSA
Journal: GEOL: Geology
DOI:10.1130/G37212.1

1 Early hydrothermal carbon uptake by the upper oceanic
2 crust: Insight from *in situ* U-Pb dating

3 Laurence A. Coogan^{1*}, Randall R. Parrish^{2,3}, and Nick M.W. Roberts³

4 ¹*School of Earth and Ocean Sciences, University of Victoria, Victoria, British Columbia*
5 *V8P 5C2, Canada*

6 ²*Department of Geology, University of Leicester and British Geological Survey,*
7 *Keyworth, Notts, NG12 5GG, UK*

8 ³*NERC Isotope Geosciences Laboratory, British Geological Survey, Keyworth, Notts,*
9 *NG12 5GG, UK*

10 *E-mail: lacoogan@uvic.ca; Tel: (1) 250 472 4018; Fax: (1) 250 721 6200

11 **ABSTRACT**

12 It is widely thought that continental chemical weathering provides the key
13 feedback that prevents large fluctuations in atmospheric CO₂, and hence surface
14 temperature, on geological timescales. However, low temperature alteration of the upper
15 oceanic crust in off-axis hydrothermal systems provides an alternative feedback
16 mechanism. Testing the latter hypothesis requires understanding the timing of carbonate
17 mineral formation within the oceanic crust. Here we report the first radiometric age
18 determinations for calcite formed in the upper oceanic crust in eight locations globally
19 via *in situ* U-Pb LA-ICP-MS analysis. Carbonate formation occurs soon after crustal
20 accretion indicating that changes in global environmental conditions will be recorded in
21 changing alteration characteristics of the upper oceanic crust. This adds support to the
22 interpretation that large differences between the hydrothermal carbonate content of Late

23 Mesozoic and Late Cenozoic oceanic crust record changes in global environmental
24 conditions. In turn, this supports a model in which alteration of the upper oceanic crust in
25 off-axis hydrothermal systems plays an important role in controlling ocean chemistry and
26 the long-term carbon cycle.

27 **INTRODUCTION**

28 Earth's long-term carbon cycle requires a negative feedback mechanism such that
29 increasing atmospheric CO₂ leads to increasing CO₂ drawdown into rocks (Berner and
30 Caldeira, 1997). The standard model has this feedback principally driven by continental
31 chemical weathering, largely through increased temperature and precipitation leading to
32 increased riverine alkalinity fluxes to the ocean and hence greater carbon draw down
33 (Berner, 2004). An alternative model suggests that the feedback is principally driven by
34 increased alteration of the upper oceanic crust (lavas) in low-temperature (10's of
35 Celcius), off-axis, hydrothermal systems (Brady and Gislason, 1997). This alternative
36 model has found recent support based on: (i) the much higher C-content of ocean crust
37 altered in the greenhouse climate of the Late Mesozoic than the icehouse climate of the
38 Late Cenozoic (Gillis and Coogan, 2011); (ii) modeling of the seawater Sr-isotope curve
39 that suggests that much of the rise in ⁸⁷Sr/⁸⁶Sr in the Late Cenozoic is due to decreasing
40 ocean temperature leading to less unradiogenic Sr being leached from the upper oceanic
41 crust (Coogan and Dosso, 2015); and (iii) modeling of the variability of seawater Mg-
42 isotopes that suggests that the Late Cenozoic increase in Mg/Ca is due to cooling
43 seawater leading to a reduced Mg sink into marine clays (Higgins and Schrag, 2015).

44 A key to testing the oceanic crust feedback model is understanding the duration
45 over which a section of oceanic crust continues to chemically interact with the ocean. In

46 detail this must depend on many local factors such as crustal permeability structure,
47 sedimentation rate and seafloor topography. However, the global average duration of
48 large-scale chemical exchange is the important factor in global geochemical cycles. For
49 example, if alteration occurs soon after crustal accretion and then largely stops, the age of
50 the crust can be used to estimate the global environmental conditions during alteration
51 and hence test predictions of this model. In contrast, if the oceanic crust continues to
52 chemically interact with the ocean over its entire lifetime, with little change in the rate of
53 chemical exchange, then environmental conditions over the entire lifetime of piece of
54 crust would have to be integrated into a model of the style of crustal alteration.

55 While previous studies have addressed the question of the timing of crustal
56 alteration (see below) here we present a novel approach to radiometrically date secondary
57 carbonate minerals for the first time. Carbonate (largely calcite except in very young
58 oceanic crust which contains abundant aragonite) is a key phase because: (i) its age
59 records the time of alkalinity generating reactions within the crust (Coogan and Gillis,
60 2013); (ii) based on textural relationships (i.e. relative ages) void filling carbonate has
61 been proposed to record the final stage of upper crust alteration in any given sample
62 (Staudigel et al., 1981; Alt and Honnorez, 1984; Gillis and Robinson, 1990); and (iii) its
63 composition has been used to track changes in ocean chemistry (Coggon et al., 2010;
64 Rausch et al., 2013) which is dependent on the assumption that carbonate forms soon
65 after crustal accretion.

66 **Sample Suite**

67 Twelve samples were selected from eight different Deep Sea Drilling Project
68 (DSDP) sites and two from the Troodos ophiolite to represent a range of crustal ages (81–

69 148 Myr) and ocean basins (Table 1 and Supplementary Information¹). Only relatively
70 old locations were selected with the aim of determining how long after crustal accretion
71 carbonate continues to form for. The samples are all from veins or, in one case, a feature
72 that could be a vein or a vug, and are from the upper 100 m of the lavas. Sample sites
73 were selected based on previous work having shown that alteration occurred at typical
74 low temperatures; this is confirmed by O-isotope data that indicate formation
75 temperatures between 9 and 23 °C similar to Cretaceous bottom water (Table 1). The
76 rationale for this was that this would lead to the largest probability that the carbonates
77 grew from typical seawater-like fluids, with high U and low Pb, giving the greatest
78 possibility of carbonate materials with high U/Pb. Of the fourteen samples, three have
79 extremely low U contents and low U/Pb making them impossible to date. These samples
80 are not discussed further although the reader should keep in mind it is possible that the
81 conclusions drawn below are only relevant to the 80% of carbonates dated.

82 **ANALYTICAL TECHNIQUES**

83 Chips of optically clean carbonate a few millimeters in size were mounted in
84 epoxy for analysis. Measurements were analogous to LA-ICP-MS methods used for
85 zircon U-Pb dating by Mottram et al. (2014) and carbonate U-Pb dating by Li et al.
86 (2014) with normalization for U-Pb and $^{207}\text{Pb}/^{206}\text{Pb}$ using the 254 Myr old WC-1 calcite
87 and NIST 614 glass, respectively. Multiple spots on a single grain were analyzed and the
88 data regressed on Tera-Wasserburg plots using Isoplot to determine the sample age (Fig.
89 1). An in-house method was used for correction of inherent variability in the proportion
90 of common lead in the WC-1 calcite. The Supplemental material¹ contains more detail on
91 methods and full data tables. Uranium contents of samples were measured by

92 normalizing the signal against that of the WC-1 calcite with an assumed ~5 ppm U
93 content, and are therefore approximate. Uncertainties of ages reflect all analytical
94 uncertainties and the uncertainty of the external standard used for normalization. Hand-
95 picked optically clean carbonate from the same samples was analyzed for O-isotopic
96 composition following the methods described in Gillis and Coogan (2011; Table 1).

97 **RESULTS**

98 Out of the eleven samples dated, the five most precise U-Pb ages (Fig. 1; Table 1)
99 are for samples from DSDP Sites 417D, 418A and 543A in the western Atlantic and Site
100 163 in the equatorial central Pacific. These samples have 2σ precisions of better than ± 5
101 Myr (ages between 82 and 128 Myr). The three samples from Sites 417D and 418A,
102 drilled within 10 km of one another, contain the highest U contents of any studied here
103 with maximum U contents ranging from 0.5 to 10 ppm (Supplementary data). The
104 samples from Sites 543A and 163 contain much lower U contents (maximum U contents
105 of 80 and 120 ppb respectively) but still have some areas with relative high U/Pb
106 allowing reasonably high precision age determinations. The data for the two samples with
107 the highest U contents show some scatter (MSWD 4.8 and 5.3; Table 1), suggesting that
108 other factors (multiple periods of growth, variable common lead isotope composition)
109 could be important; the uncertainties take account of the scatter in regressions but their
110 absolute uncertainties need to be used with some caution. Three samples have
111 intermediate age uncertainties of ± 5 –10 Myr (Fig. 1). These samples have maximum U
112 contents ranging from 50 to 80 ppb but Pb contents generally <5 ppb allowing reasonably
113 precise ages. The three samples with the largest uncertainties (± 10 –20 Myr) are from
114 DSDP Site 595B (two samples) and the Troodos ophiolite; these samples contain <40

115 ppb U. For all of these samples there are no analyses with low common lead and hence
116 there is a large extrapolation from the array of data to the concordia age intercept and the
117 uncertainties quoted should be considered as minimum values.

118 The new carbonate formation ages (Fig. 1; Table 1) provide the first direct
119 determination of whether carbonate formation occurs soon after crustal accretion or
120 throughout the life of a section of oceanic crust – both of which have been previously
121 suggested (Staudigel and Hart, 1985; Alt and Teagle, 1999; Gillis and Coogan, 2011;
122 Coogan and Dosso, 2015). Despite the analytical challenges in dating these materials it is
123 clear that most carbonate forms soon after crustal accretion (Fig. 2); this interpretation is
124 consistent with other preliminary data, collected in the same way, recently reported by
125 Harris et al. (2014). Notably, none of the carbonate ages are >20 Myr younger than the
126 crust despite all the study areas being in >80 Myr old crust. While fluid and heat fluxes
127 are not expected to directly match chemical fluxes, it is notable that >80% of the off-axis
128 hydrothermal heat flux is removed within 20 Myr of crustal accretion.

129 **DISCUSSION**

130 **Conditions in the Aquifer During Carbonate Growth**

131 Carbonate mineral precipitation in the upper oceanic crust occurs largely in
132 response to fluid-rock reactions that generate alkalinity and hence increase the saturation
133 state of carbonate minerals (Coogan and Gillis, 2013). Heterogeneity in the U and Pb
134 contents of the carbonates (Fig. 1; Supplementary material¹) suggests that the
135 concentrations of U and Pb in the aquifer fluid, and/or environmental conditions (pH,
136 redox, T), varied during carbonate growth. Formation of secondary minerals at low
137 temperatures adds U to the crust (e.g., Staudigel et al., 1995) and will lead to decreasing

138 U contents of the aquifer fluid as fluid-rock reaction progresses, at least partial explaining
139 the observed variability in U/Pb. This fluid-rock reaction occurs despite the low
140 carbonate formation temperatures (9–23 °C; Table 1). Such modification of the fluid
141 composition, on timescales shorter than that of the growth of a single carbonate vein,
142 needs careful consideration when interpreting past compositions of seawater from the
143 compositions of carbonate minerals precipitated within the oceanic crust (e.g., Coggon et
144 al., 2010; Rausch et al., 2013).

145 Modern deep seawater contains very little Pb (~2 ppt; Bruland et al., 2014) and
146 has a high U/Pb (~1000) and fluids entering the crustal aquifer have probably had
147 similarly high U/Pb throughout the Phanerozoic. The low Pb content of seawater, and its
148 short residence time, means that the Pb-isotopic composition of seawater can vary on
149 short timescales (kyr). Thus, variations in the Pb content, and isotopic composition, of the
150 aquifer fluid during the growth of a carbonate vein may be caused by either: (i) changing
151 seawater Pb content/isotopic composition, and/or (ii) fluid-lava or fluid-sediment
152 reactions; i.e., no additional source of Pb is required by the Pb-isotope variability
153 although it cannot be ruled out.

154 The excess scatter of the data about a linear correlation (i.e., MSWD >2.0 at 2σ)
155 between $^{238}\text{U}/^{206}\text{Pb}$ and $^{207}\text{Pb}/^{206}\text{Pb}$ in some samples (Fig. 1) most likely reflects either: (i)
156 varying Pb-isotopic composition of the fluid that the carbonate grew from, (ii) protracted
157 carbonate growth and/or (iii) analytical factors difficult to correct for in low-signal
158 analyses. Protracted growth of carbonates, perhaps over millions of years, may be a
159 natural consequence of the large fluid fluxes required to supply sufficient C to the crust to
160 form the mass of carbonate observed in some drill cores (Coogan and Gillis, 2013).

161 **Low-Temperature Alteration Occurs Early**

162 It is clear from the new data reported here that most carbonate precipitation within
163 the upper oceanic crust occurs within the first 20 Myr after crustal formation (>80%;
164 Figure 2, 3). Our samples come from a wide range of locations and from crust with ages
165 between 80 and 148 Myr but none of the carbonates ages are >16 Myr younger than the
166 crustal age. The only previous approach to determining the timing of carbonate formation
167 in the ocean crust compares the Sr-isotopic compositions of carbonates with the seawater
168 Sr-isotope curve. This approach gives a non-unique result both because the seawater
169 curve shows fluctuations in $^{87}\text{Sr}/^{86}\text{Sr}$, and because basalt dissolution lowers the $^{87}\text{Sr}/^{86}\text{Sr}$
170 of crustal fluids. Early qualitative approaches concluded that carbonates were precipitated
171 within 10–15 Myr of crustal accretion assuming no basaltic Sr in the fluid (Staudigel and
172 Hart, 1985). More recent quantitative models show that the data can be explained with an
173 exponentially decreasing rate of carbonate precipitation with 85% of carbonate
174 precipitated within <20 Myr of crustal accretion (Gillis and Coogan, 2011; Coogan and
175 Dosso, 2015). The good agreement between the model ages and the direct age
176 determinations presented here (Fig. 3) suggest that the assumptions inherent in the Sr-
177 isotope model ages are reasonable.

178 It is useful to compare the U-Pb age distribution of carbonates with previous
179 radiometric age determinations for other low temperature alteration minerals formed in
180 the upper ocean crust. The most robust data sets come from K-Ar and Rb-Sr dating of
181 celadonite with just a few alteration age determinations from Rb-Sr isochron ages that
182 include clays and zeolites. Existing K-Ar ages of alteration of upper ocean crust come
183 almost entirely from celadonites in the Troodos ophiolite (54 samples from Gallahan and

184 Duncan, 1994, and 4 from Staudigel et al., 1986). Comparison of these K-Ar ages to Rb-
185 Sr ages of 18 of the same celadonites suggests that they may have suffered some Ar-loss,
186 with Rb-Sr dates generally older (by a maximum of 14 Myr and an average of 5 Myr;
187 Booij et al., 1995). Celadonite formation as a function of time after crustal accretion
188 follows a similar pattern to carbonate formation although perhaps offset toward forming
189 slightly later (Fig. 3); this probably simply reflects different sample suites rather than a
190 real difference in the timing of carbonate and celadonite formation. Likewise, the limited
191 existing isochron age determinations of ocean crust alteration suggest this occurs soon
192 after crustal accretion (e.g., Richardson et al., 1980; Staudigel et al., 1986). Thus it seems
193 clear that, in general, the vast majority of the low temperature alteration of the upper
194 oceanic crust occurs within 20 Myr of crustal accretion (Fig. 3).

195 Several studies have suggested that carbonates are the last phases to form during
196 off-axis alteration of the upper oceanic crust (Staudigel et al., 1981; Alt and Honnorez,
197 1984; Gillis and Robinson, 1990). This is difficult to reconcile with the need for
198 alkalinity generating fluid-rock reaction to drive carbonate precipitation because these
199 must be accompanied by the formation of secondary silicates. The new age data suggest
200 carbonates and secondary silicates form over the same time interval (largely in the first
201 20 Myr after crustal accretion) resolving this paradox.

202 **Implications for the Regulation of Ocean Chemistry**

203 The relatively rapid alteration of new upper oceanic crust (Fig. 2, 3) has important
204 implications for testing whether low-temperature alteration of the oceanic crust plays an
205 important role in the feedback mechanisms that regulate ocean chemistry and the long-
206 term carbon cycle. If this model is correct then, on a timescale of 10–20 million years

207 (i.e. the timescale of the majority of chemical exchange), there should be a correlation
208 between the composition of altered oceanic crust and the global environmental
209 conditions. The higher C content of Cretaceous than Cenozoic altered upper oceanic crust
210 supports a model of increased alkalinity production during periods of globally warm
211 conditions (Gillis and Coogan, 2011). This model also makes predictions for the average
212 change in Sr and Mg isotopic composition of upper ocean crust of different ages (Coogan
213 and Dosso, 2015; Higgins and Schrag, 2015), as well as other element and isotope
214 systems. However, we caution that local crustal hydrological conditions will have to be
215 considered to ensure a signal relevant to global fluxes is extracted from such data.

216 **ACKNOWLEDGMENTS**

217 Reviews by Hubert Staudigel and John Higgins helped improve the manuscript.
218 Kathy Gillis provided some of the samples analyzed here and critical comments. We
219 thank T. Rasbury for the WC-1 calcite.

220 **REFERENCES CITED**

- 221 Alt, J.C., and Honnorez, J., 1984, Alteration of the upper oceanic crust, DSDP Site 417:
222 mineralogy and chemistry: *Contributions to Mineralogy and Petrology*, v. 87,
223 p. 149–169, doi:10.1007/BF00376221.
- 224 Alt, J.C., and Teagle, D.A.H., 1999, The uptake of carbon during alteration of ocean
225 crust: *Geochimica et Cosmochimica Acta*, v. 63, p. 1527–1535, doi:10.1016/S0016-
226 7037(99)00123-4.
- 227 Berner, R.A., 2004, *The Phanerozoic carbon cycle*: Oxford, New York, Oxford
228 University Press.

- 229 Berner, R.A., and Caldeira, K., 1997, The need for mass balance and feedback in the
230 geochemical carbon cycle: *Geology*, v. 25, p. 955–956, doi:10.1130/0091-
231 7613(1997)025<0955:TNFMBA>2.3.CO;2.
- 232 Booij, E., Gallahan, W.E., and Staudigel, H., 1995, Ion-exchange experiments and Rb/Sr
233 dating on celadonites from the Troodos ophiolite, Cyprus: *Chemical Geology*, v.
234 126, p. 155–167, doi: [http://dx.doi.org/10.1016/0009-2541\(95\)00116-1](http://dx.doi.org/10.1016/0009-2541(95)00116-1).
- 235 Brady, P.V., and Gislason, S.R., 1997, Seafloor weathering controls on atmospheric CO₂
236 and global climate: *Geochimica et Cosmochimica Acta*, v. 61, p. 965–973,
237 doi:10.1016/S0016-7037(96)00385-7.
- 238 Bruland, K.W., Middag, R., and Lohan, M.C., 2014, Controls of Trace Metals in
239 Seawater, *in* Turekian, H.D., and Holland H.K., eds., *Treatise on Geochemistry* (2nd
240 edition): Oxford, Elsevier, p. 19–51, doi:10.1016/B978-0-08-095975-7.00602-1.
- 241 Coggon, R.M., Teagle, D.A.H., Smith-Duque, C.E., Alt, J.C., and Cooper, M.J., 2010,
242 Reconstructing Past Seawater Mg/Ca and Sr/Ca from Mid-Ocean Ridge Flank
243 Calcium Carbonate Veins: *Science*, v. 327, p. 1114–1117,
244 doi:10.1126/science.1182252.
- 245 Coogan, L.A., and Dosso, S.E., 2015, Alteration of ocean crust provides a strong
246 temperature dependent feedback on the geological carbon cycle and is a primary
247 driver of the Sr-isotopic composition of seawater: *Earth and Planetary Science*
248 *Letters*, v. 415, p. 38–46, doi:10.1016/j.epsl.2015.01.027.
- 249 Coogan, L.A., and Gillis, K.M., 2013, Evidence that low-temperature oceanic
250 hydrothermal systems play an important role in the silicate-carbonate weathering

- 251 cycle and long-term climate regulation: *Geochemistry Geophysics Geosystems*,
252 v. 14, p. 1771–1786, doi:10.1002/ggge.20113.
- 253 Epstein, S., Buchsbaum, R., Lowenstam, H.A., and Urey, H.C., 1953, Revised carbonate-
254 water isotopic temperature scale: *Geological Society of America Bulletin*, v. 64, p.
255 1315–1325, doi: 10.1130/0016-7606(1953)64[1315:RCITS]2.0.CO;2.
- 256 Gallahan, W.E., and Duncan, R.A., 1994, Spatial and temporal variability in
257 crystallization of celadonites within the Troodos ophiolite, Cyprus: Implications for
258 low-temperature alteration of the oceanic crust: *Journal of Geophysical Research*,
259 v. 99, p. 3147–3161, doi:10.1029/93JB02221.
- 260 Gillis, K.M., and Coogan, L.A., 2011, Secular variation in carbon uptake into the ocean
261 crust: *Earth and Planetary Science Letters*, v. 302, p. 385–392,
262 doi:10.1016/j.epsl.2010.12.030.
- 263 Gillis, K.M., and Robinson, P.T., 1990, Patterns and processes of alteration in the lavas
264 and dykes of the Troodos Ophiolite, Cyprus: *Journal of Geophysical Research*, v. 95,
265 p. 21,523–21,548, doi:10.1029/JB095iB13p21523.
- 266 Harris, M., Coggon, R.M., Teagle, D.A.H., Roberts, N.M.W., and Parrish, R.R., 2014,
267 Laser ablation MC-ICP-MS U/Pb geochronology of ocean basement calcium
268 carbonate veins: Abstract V31B–4740 presented at 2014 Fall Meeting, AGU, San
269 Francisco, California, 15–19 December.
- 270 Higgins, J.A., and Schrag, D.P., 2015, The Mg isotopic composition of Cenozoic
271 seawater – evidence for a link between Mg-clays, seawater Mg/Ca, and climate:
272 *Earth and Planetary Science Letters*, v. 416, p. 73–81,
273 doi:10.1016/j.epsl.2015.01.003.

- 274 Li, Q., Parrish, R.R., Horstwood, M.S.A., and McArthur, J.M., 2014, U-Pb dating of
275 cements in Mesozoic ammonites: *Chemical Geology*, v. 376, p. 76–83,
276 doi:10.1016/j.chemgeo.2014.03.020 (erratum available at
277 <http://dx.doi.org/10.1016/j.chemgeo.2014.07.005>).
- 278 Mottram, C.M., Argles, T.W., Harris, N.B.W., Parrish, R.R., Horstwood, M.S.A.,
279 Warren, C.J., and Gupta, S., 2014, Tectonic interleaving along the Main Central
280 Thrust, Sikkim Himalaya: *Journal of the Geological Society*, v. 171, p. 255–268,
281 doi:10.1144/jgs2013-064.
- 282 Rausch, S., Boehm, F., Bach, W., Kluegel, A., and Eisenhauer, A., 2013, Calcium
283 carbonate veins in ocean crust record a threefold increase of seawater Mg/Ca in the
284 past 30 million years: *Earth and Planetary Science Letters*, v. 362, p. 215–224,
285 doi:10.1016/j.epsl.2012.12.005.
- 286 Richardson, S.H., Hart, S.R., and Staudigel, H., 1980, Vein mineral ages of old oceanic
287 crust: *Journal of Geophysical Research*, v. 85, p. 7195–7200,
288 doi:10.1029/JB085iB12p07195.
- 289 Staudigel, H., and Hart, S.R., 1985, Dating of ocean crust hydrothermal alteration:
290 Strontium isotope ratios from Hole 504B carbonates and reinterpretation of Sr
291 Isotope data from Deep Sea Drilling Project Sites 105, 332, 417, and 418: *in*
292 Anderson, R.N., Honnorez, J., and Becker, K., eds., *Initial Reports of the Deep Sea*
293 *Drilling Project*, Washington, DC., US Government Printing Office, vol. 83, p. 297–
294 303.

- 295 Staudigel, H., Hart, S.R., and Richardson, S.H., 1981, Alteration of the Oceanic-Crust -
296 Processes and Timing: Earth and Planetary Science Letters, v. 52, p. 311–327,
297 doi:10.1016/0012-821X(81)90186-2.
- 298 Staudigel, H., Gillis, K., and Duncan, R., 1986, K/Ar and Rb/Sr ages of celadonites from
299 the Troodos ophiolite, Cyprus: Geology, v. 14, p. 72–75, doi:10.1130/0091-
300 7613(1986)14<72:AASAOC>2.0.CO;2.
- 301 Staudigel, H., Davies, G.R., Hart, S.R., Marchant, K.M., and Smith, B.M., 1995, Large
302 scale isotopic Sr, Nd and O isotopic anatomy of altered oceanic crust: DSDP/ODP
303 sites417/418: Earth and Planetary Science Letters, v. 130, p. 169–185,
304 doi:10.1016/0012-821X(94)00263-X.

305

306 FIGURE CAPTIONS

307

308 Figure 1. Tera-Wasserburg concordia plots showing $^{238}\text{U}/^{206}\text{Pb}$ versus $^{207}\text{Pb}/^{206}\text{Pb}$ (age
309 and uncertainty are show in the title). The samples are ordered such that the more precise
310 ages are in the upper row and the least precise ages in the lower row.

311

312 Figure 2. Comparison of the measured carbonated age and the estimated age of the crust
313 the carbonate came from. Considering the errors associated with both ages, the carbonate
314 and crustal ages are virtually identical (gray symbols are samples shown in the lower row
315 in Fig. 1, with large extrapolations to the age intercept). The inset shows the same but
316 with the axes starting at zero, the time of sampling, showing more clearly that although
317 the carbonates could, theoretically, have formed at any time after crustal accretion (i.e.,

318 vertically down from the 1:1 line in the gray polygon) they actually formed very soon
319 after crustal accretion.

320

321 Figure 3. Comparison of the cumulative fraction of secondary minerals formed by low
322 temperature alteration of the upper oceanic crust as a function of time after crustal
323 accretion based on carbonate U-Pb ages (this study), celadonite K-Ar ages (Gallahan and
324 Duncan, 1994; Staudigel et al., 1986), celadonite Rb-Sr ages (Booij et al., 1995) and
325 carbonate Sr-isotopic composition modeling (Coogan and Dosso, 2015). The probability
326 distribution for each age determination was summed across all samples, accounting for
327 the individual age uncertainties, and the positive portion of this used to calculate the
328 cumulative frequency. In cases where the measured age distribution includes time before
329 crustal accretion these were normalized out of the probability distribution; this is only of
330 any significance for the U-Pb carbonate ages.

331

332 ¹GSA Data Repository item 2015xxx, [this provides further background on the sample
333 sites and analytical techniques as well as all the full dataset], is available online at
334 www.geosociety.org/pubs/ft2009.htm, or on request from editing@geosociety.org or
335 Documents Secretary, GSA, P.O. Box 9140, Boulder, CO 80301, USA.

336

337

338

339

340

341

342

343

344

345

346
 347
 348
 349
 350
 351
 352
 353

TABLE 1: CARBONATE COMPOSITIONS AND AGES

Sample	Texture	Crustal age (Myr)	Ave U (ppb)	Ave Pb (ppb)	Age	MSWD	$^{207}\text{Pb}/^{206}\text{Pb}_{(i)}$	$\delta^{13}\text{C}$ (VPDB) ^b	$\delta^{18}\text{O}$ (SMOW) ^b	Formation temp. (°C)
595B-2R1-84-95*	vein	95	13	3.5	115 ± 16	1.5	0.87 ± 0.01	2.6	30.5	14.0
595B-3R2-12-18*	vein	95	19	2.1	86 ± 14	6.6	0.85 ± 0.02	2.4	30.2	15.0
543-16R6-114.5-118*	vug/vein	80.8	50	3.7	91.3 ± 4.9	1.5	0.87 ± 0.01	2.5	30.9	12.5
543-16R6-114.5-118D	vug/vein	80.8						3.0	30.9	12.3
163-29R5-0	vein	80.8	91	9.1	81.5 ± 3.3	1.15	0.85 ± 0.01	2.9	31.9	8.7
164-28R3-23	vein	109	32	1.8	117.6 ± 9.6	0.42	0.83 ± 0.03	2.7	29.9	16.6
164-28R4-44	vein	109	33	4.9	115.6 ± 5.4	1.07	0.84 ± 0.01	1.7	28.5	22.4
417D-27R4-61	vein	120	124	3.6	103.9 ± 3.1	0.31	0.83 ± 0.01	1.8	30.2	15.4
417D-31R4-8	vein	120	2457	49	127.5 ± 4.7	5.3	0.86 ± 0.05	1.6	28.4	22.9
418A-15R3-144	vein	119.9	534	18	121.9 ± 4.7	4.8	0.85 ± 0.03	2.5	29.1	19.8
307 13R2 145	vein	148.3	63	2.4	142.8 ± 8.6	0.9	0.83 ± 0.03	1.1	29.4	18.4
2012CL26	vein	91.6	19	4.4	105 ± 19	1.7	0.89 ± 0.02	1.5	31.9	8.5
2012CL26D	vein	91.6						1.5	31.9	8.5

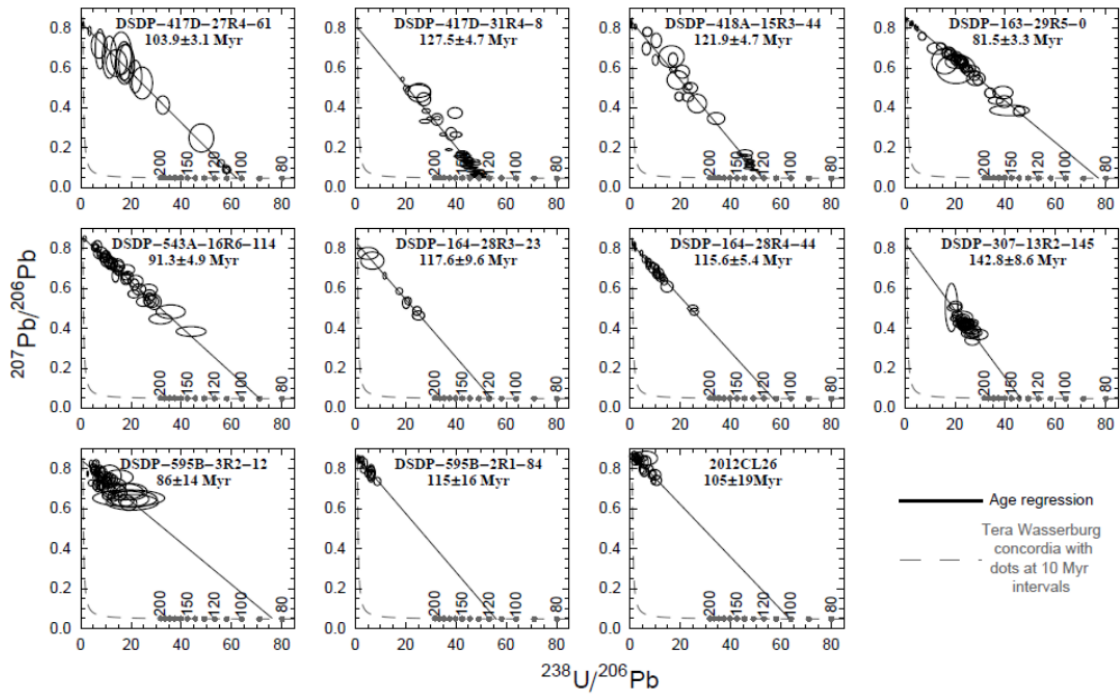
Note: We arbitrarily assign a ± 2 Myr uncertainty to all crustal ages except DSDP Site 595 for which the uncertainty is clearly larger and we assign ± 10 Myr (Supplementary material). D - duplicate analysis. Formation temperatures are calculated assuming a fluid $\delta^{18}\text{O}$ of -1 per mil and using the thermometer of Epstein et al. (1953)

i—intercept

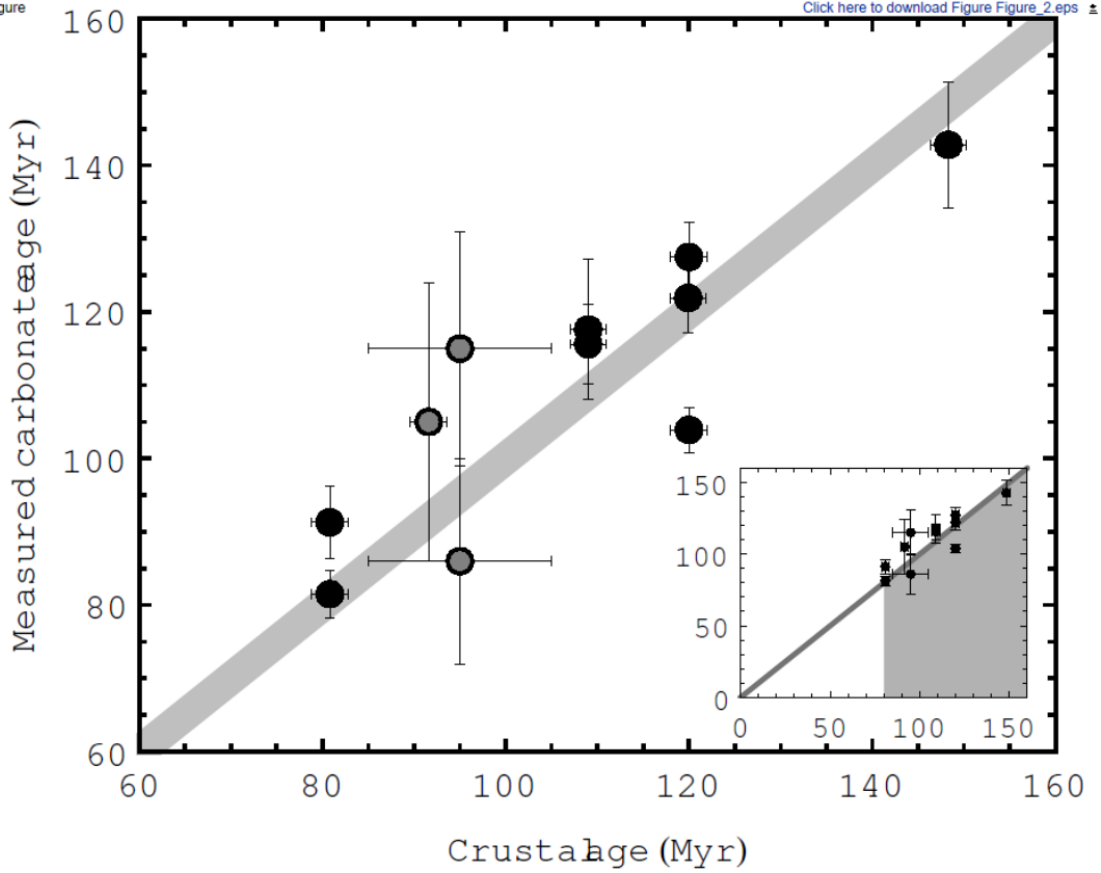
^bO and C isotopes data from Gillis and Coogan (2011).

354
 355
 356
 357
 358
 359

360 Figure1:

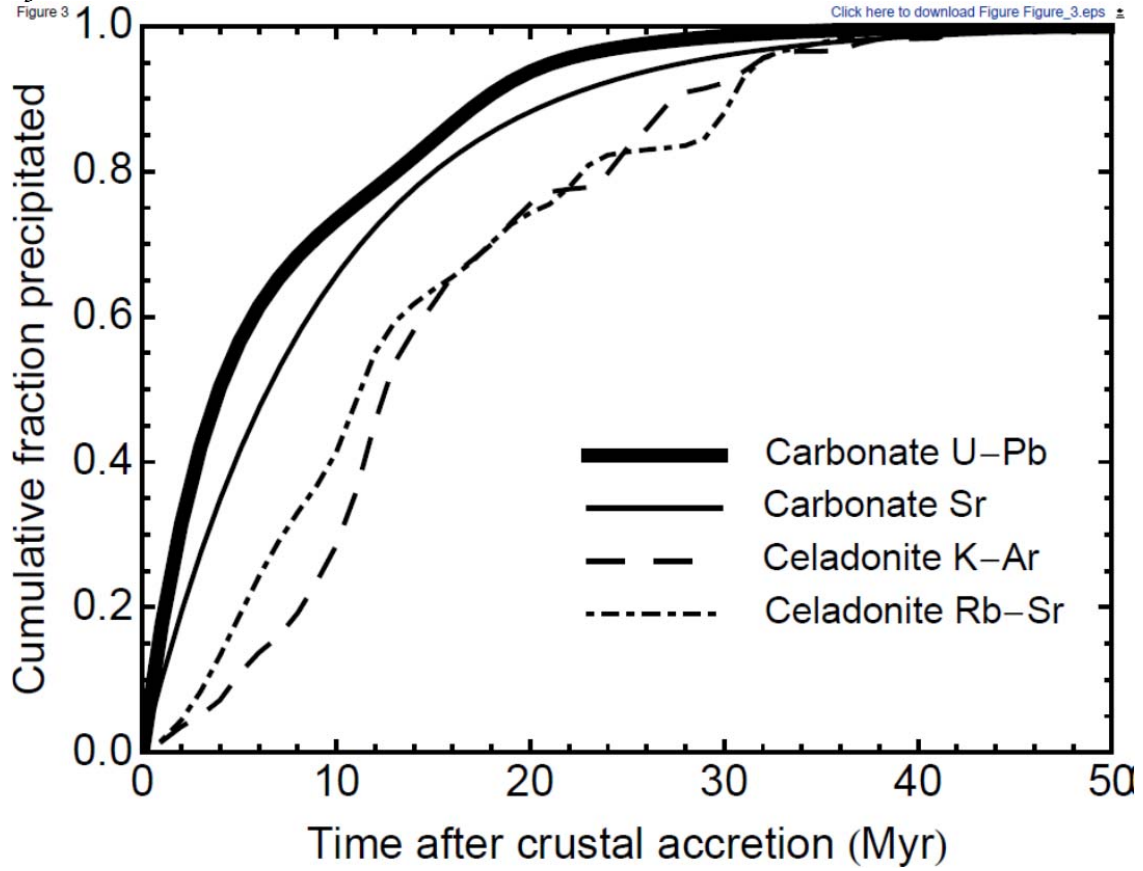


361
 362
 363 Figure2:
 Figure



364

365 Figure 3:
Figure 3



366
367
368
369
370
371